The MSHT20 parton distribution functions

R.S. Thorne[1⋆], S. Bailey[2], T. Cridge[1], L.A. Harland-Lang [2] and A.D. Martin[3]

1 Department of Physics and Astronomy, University College London, London, WC1E 6BT, UK
2 Rudolf Peierls Centre, Beecroft Building, Parks Road, Oxford, OX1 3PU
3 Institute for Particle Physics Phenomenology, Durham University, Durham, DH1 3LE, UK

⋆ robert.thorne@ucl.ac.uk

Proceedings for the XXVIII International Workshop on Deep-Inelastic Scattering and Related Subjects, Stony Brook University, New York, USA, 12-16 April 2021
doi:10.21468/SciPostPhysProc.8

Abstract

We present the new MSHT20 set of parton distribution functions (PDFs) of the proton, determined from a global analysis of the available hard scattering data and superseding the MMHT14 sets. The parameterisation is now adapted and extended and we include a large number of new data sets: the final HERA and Tevatron data, and a significant number of LHC data sets on vector boson production, inclusive jets and top quark distributions. We include up to NNLO QCD corrections for all data sets that play a major role in the fit. There are some changes to central PDF values and a significant reduction in the uncertainties, but the PDFs and the predictions using them are generally within one standard deviation of the MMHT14 results. We discuss the phenomenological impact of our results.

Received 27-07-2021
Accepted 28-02-2022
Published 11-07-2022
doi:10.21468/SciPostPhysProc.8.018

1 Introduction

We summarise the most important results pertaining to the MSHT20 PDFs [1]. The acronym MSHT stands for Mass Scheme Hessian Tolerance, i.e. it incorporates some of the central and enduring features of our approach, and is now intended to be a permanent naming convention. The 2020 analysis includes new theoretical developments, and an extended parameterisation – particularly for $\bar{d}/\bar{u}$ and the strange quark – and eigenvector sets. There is the addition of much new, largely LHC data, but also HERA and Tevatron data sets. Nearly all cross sections are included at NNLO in QCD perturbation theory. The fit quality is generally very good, but there are problems with correlated uncertainties and tensions for some data sets. NNLO is now very much the default, and NLO QCD is clearly no longer sufficient for real precision. The new PDFs join the list of others recently obtained via global fits [2–4].

2 Theoretical Procedures

As in the MMHT14 [5] analysis we use a general mass variable flavour scheme based on the TR scheme [6,7], using the "optimal" choice [8] for smoothness near threshold. We use deuteron and heavy nuclear corrections, the former fit using a 4 parameter model, as in MMHT14 and the latter use the same corrections [9] as MMHT14 with the fit allowing an additional penalty-free freedom of order 1%. We fit data with systematic uncertainties using either nuisance parameters if possible (the preferred method) or with the correlation matrix provided, and use statistical correlations whenever these are available. (Some old data sets which are dominated by uncorrelated uncertainties and/or where there is a limited understanding of correlations have errors added in quadrature.) We fit to absolute cross sections in preference to normalized to avoid loss of information from normalizations.

The analysis includes many new NNLO corrections compared to MMHT14. We now use the NNLO calculations for dimuon production [10], where the correction is negative, but larger in size at lower x. This negative correction allows the strange quark to be larger in the fit to the dimuon data and helps relieve tension between the dimuon data [11] and LHC W,Z data [12–14] which prefers a larger strange quark [15], as seen in Fig. 1.

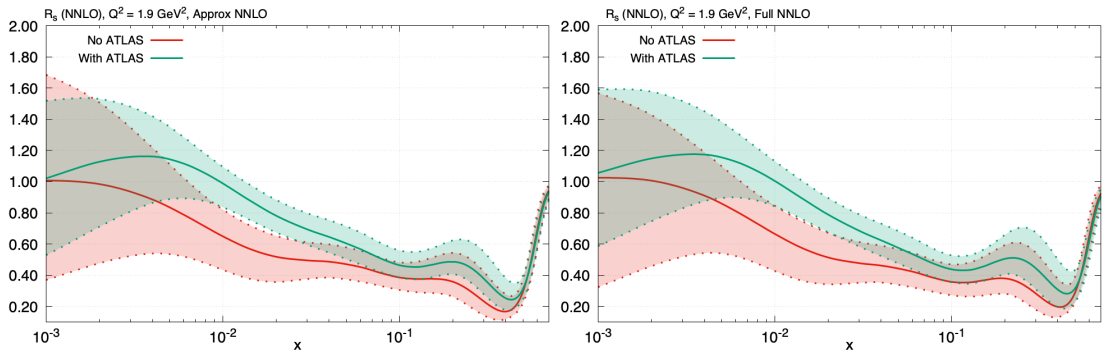

Figure 1: The ratio of strange quarks to light quarks in fits without (left) and with (right) the full NNLO corrections.

Nearly all other data have the theoretical calculations at full NNLO precision. In particular we also include NNLO cross-section calculations [16] for all LHC jet data, i.e. we fit inclusive jet production at 2.76, 7 and 8 TeV, using the larger available jet radius, e.g. $R = 0.6, 0.7$ and scales $\mu_{R,F} = p_{T,jet}$. (Older Tevatron jet data are still included with the threshold approx for NNLO [17] - which is a better approximation for these data which also carry little weight.) CMS 7 TeV $W+c$ data [18] only have NLO theory available for the specific measurement, but the correction is not expected to be large compared to the uncertainties and the few data points carry little weight. The Zp_T distribution and all top quark cross sections used are included at full NNLO. We also use EW corrections where possible, if these are not already subtracted from the data supplied.

There has been a very significant extension of our parameterisation. In MMHT14 the general parameterisation used for PDFs was $A(1-x)^\eta x^\delta(1+\sum_{i=1}^{n} a_i T_i(1-2x^{1/2}))$, where $T_i(1-2x^{1/2})$ are Chebyshev polynomials. It was shown in [19] how the achieved precision possible improved with increasing n using a fit to pseudo-data. In MMHT14 $n=4$ was deemed sufficient, but using $n=6$ will lead to much better than 1% precision. Hence, we have investigated extending the parameters of different flavour PDFs sequentially using $n=6$ and also, now parameterise $(\bar{d}/\bar{u})$ instead of $(\bar{d}-\bar{u})$, with the sole constraint that $(\bar{d}/\bar{u}) \to$ constant as $x \to 0$. This leads to significant improvements in the global fit: changing to $(\bar{d}/\bar{u})(x,Q_0^2)$ gave $\Delta\chi^2_{tot} = -18$; additionally extending $d_V(x,Q_0^2)$ gave $\Delta\chi^2_{tot} \sim -32$; extending $u_V(x,Q_0^2)$

was not significant but further extending $g(x,Q_0^2)$ gave $\Delta\chi^2_{tot} \sim -50$; and finally extending $sea(x,Q_0^2)$ and $s^+(x,Q_0^2)$ gave $\Delta\chi^2_{tot} = -73$. Overall we see an improvement in the fit to high-x fixed-target data, a reduction in tension between E866 DY ratio data and LHC data, and an improvement in the description of the LHC lepton asymmetry data, while the gluon-induced improvement is in HERA and other data. Using $n = 6$ in general now, except for $s - \bar{s}$, means an increase to 52 parton parameters.

3 New Data Sets

The first new data set to be updated compared to the MMHT14 PDFs was the final HERA total cross section data [20]. This was already studied in [21] and found to have a limited effect on the PDFs, but there was some trouble fitting the lower Q^2, x data. We now also include final combined $\tilde{\sigma}^{\bar{c}c}$ and $\tilde{\sigma}^{\bar{b}b}$ data [22]. The best fit is $\chi^2 = 132/79$, quite high but there is no tension with other data within the global fit, except the inclusive HERA data which carries enormously more weight on the relevant PDFs. The fit at low Q^2 is not optimal, but similar results are seen in other PDF studies [22].

Another important additional new data set is D0 electron/W asymmetry. We first fit D0 e asymmetry [23], and found good agreement with MMHT14, but alternatively we can use W-asymmetry [24]. The $W^{+/-}$ boson is produced preferentially in the proton/antiproton direction, but the V–A structure of the lepton decay means $e^{+/-}$ is emitted preferentially opposite to $W^{+/-}$ – leptons at particular η^e come from a range of η^W values and dilute the direct constraint on PDFs at given x. Mapping the lepton to W asymmetry requires PDF-dependent modelling, with a small uncertainty and this gives a more direct constraint from W asymmetry data. We see a reduced uncertainty on d/u compared to using the e asymmetry. There is a marked effect at very high x, where d_V is reduced, see Fig. 2.

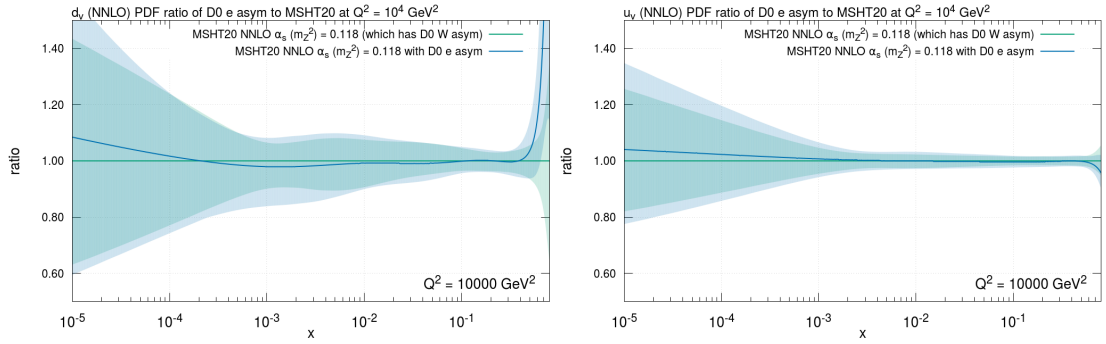

Figure 2: The effect of inclusion of D0 W asymmetry data compared to e asymmetry data for d_v (left) and u_V (right).

The MSHT20 analysis contains a large amount of new LHC data: extremely high precision data on W, Z at 7 TeV from ATLAS, and high precision $W^{+/-}$ data and double differential Z data at 8 TeV; CMS 8 TeV precise data on the $W^{+,-}$ rapidity distribution; LHCb data at 7 and 8 TeV on W, Z rapidity distributions at higher rapidity; $W+c$ jets data at 7 TeV from CMS; ATLAS high mass Drell Yan data at 8 TeV; ATLAS data on $W^{+/-}$ + jets at 8 TeV; Z p_T distributions at 8 TeV; new data on $\sigma_{t\bar{t}}$ at 8 TeV plus ATLAS single differential distributions in $p_{T,t}, M_{t\bar{t}}, y_t, y_{t\bar{t}}$ and CMS double differential distributions in $p_{T,t}, y_t$ both at 8 TeV; inclusive jet data from ATLAS at 7 TeV and CMS at 2.76, 7 and 8 TeV. We include all these recent LHC data updates in the fit at NNLO (for default $\alpha_S(M_Z^2) = 0.118$). The fit quality is generally good, as seen in Table 1. There are relatively poor χ^2 values for some sets seemingly observed by other groups.

The main effect of the new LHC data on PDFs is on the details of flavour, i.e. the d_V shape,

	no. points	NNLO $\chi^2/N_{\rm pts}$
D0 W asymmetry [24]	14	0.86
$\sigma_{t\bar{t}}$ Tevatron +CMS+ATLAS 7, 8 TeV [25]- [26]	17	0.85
LHCb 7+8 TeV $W+Z$ [27,28]	67	1.48
LHCb 8 TeV e [29]	17	1.54
CMS 8 TeV W [30]	22	0.58
ATLAS 7 TeV jets $R=0.6$ [31]	140	1.59
CMS 7 TeV $W+c$ [18]	10	0.86
ATLAS 7 TeV W,Z [12]	61	1.91
CMS 7 TeV jets $R=0.7$ [32]	158	1.11
ATLAS 8 TeV Zp_T [33]	104	1.81
CMS 8 TeV jets [34]	174	1.50
ATLAS 8 TeV $t\bar{t}\to l+$j single-diff [35]	25	1.02
ATLAS 8 TeV $t\bar{t}\to l^+l^-$ single-diff [36]	5	0.68
ATLAS 8 TeV high-mass Drell-Yan [37]	48	1.18
ATLAS 8 TeV $W^{+,-}+$jet [38]	32	0.60
CMS 8 TeV $(d\sigma_{t\bar{t}}/dp_{T,t}dy_t)/\sigma_{t\bar{t}}$ [39]	15	1.50
ATLAS 8 TeV W^+,W^- [13]	22	2.61
CMS 2.76 TeV jets [40]	81	1.27
CMS 8 TeV $t\bar{t}$ y_t distribution [41]	9	1.47
ATLAS 8 TeV double differential Z [14]	59	1.45
Total, LHC data	1328	1.33
Total, all data	4363	1.17

Table 1: The χ^2 for new collider data in the MSHT20 fit.

an increase in the strange quark for $0.001 < x < 0.3$ and the $\bar{d},\bar{u}$ details, though some of these are also partially from the parameterisation change. There is a slight decrease in the high-x gluon. We will illustrate these changes later. Generally the fit is good, but the most straightforward approach gives a distinctly poor fit quality to some data sets due to tensions between different kinematic regions (e.g. rapidity bins) or different differential distributions of the same data. Sometimes this is clearly related to modelling-type systematic uncertainties, particularly for jet and $t\bar{t}$ data, as illustrated in detail in [42, 43], and for some data sets we use the sort of smooth decorrelation advocated for 8 TeV ATLAS inclusive jet data [44].

4 The new PDFs

When determining the PDF uncertainties in MSHT20 we go from 25 eigenvector pairs to 32 - there is one extra parameter for each PDF and two for $s+\bar{s}$. The mean tolerance is $T\sim 3-4$. About half the constraints are primarily provided by precision electroweak collider data, largely D0 W asymmetry, 7 TeV and 8 TeV ATLAS W,Z and CMS W data. 8-10 eigenvectors are mainly constrained by the E866 Drell-Yan ratio which is vital for the $\bar{d}/\bar{u}$ constraint, ~ 10 eigenvectors are constrained by fixed target DIS data (i.e. BCDMS, NMC, NuTeV, CCFR) and these data sets still mainly constrain high-x quarks, ~ 10 eigenvectors are constrained by CCFR, NuTeV dimuon data, i.e. this is still the main constraint on the strange quark and its asymmetry. Hence, a fully global fit is necessary for a full constraint on all PDFs without use of assumptions and/or models. HERA data provides good constraints on the widest variety of PDF parameters, mainly the gluon and light sea, but now is very rarely the best. However the HERA data are a very strong constraint on the best fit PDFs, and central values and uncertainties at small x are strongly constrained by HERA data as seen in Fig. 3, and the quark normalization at high-x is also affected - which is related to sum rules.

We now consider the new MSHT20 PDFs compared to those of MMHT14. First we show the gluon distribution, Fig. 4 (left), where there is no significant change in the central value, though the uncertainty is reduced. The details in shape at high x depend on the LHC jet, $Z\,p_T$ and differential $t\bar{t}$ data. The $Z\,p_T$ data pull the gluon up and differential $t\bar{t}$ data pulls the gluon down, each also affecting the lower x normalization via the momentum sum rule. This is seen in Fig. 4 (right). Not all jet data pull in the same direction though the total effect is slightly downwards.

More significant changes in the PDFs include an increase in the strange quark below

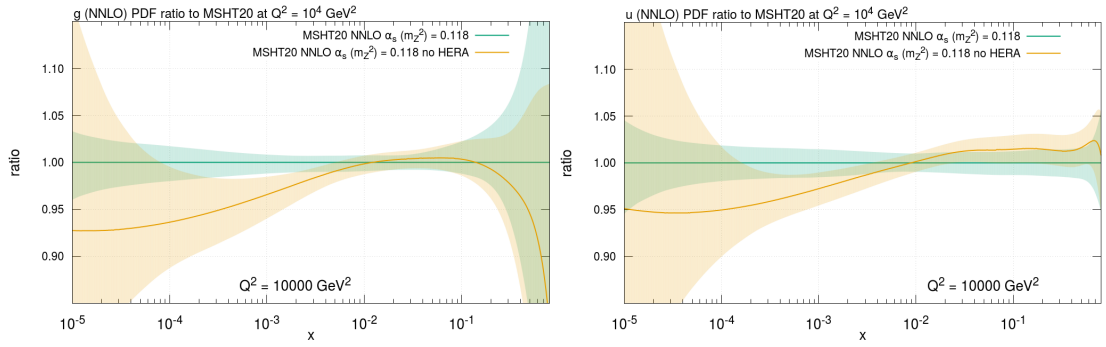

Figure 3: PDFs with and without inclusion of HERA data for gluon (left) and up quark (right).

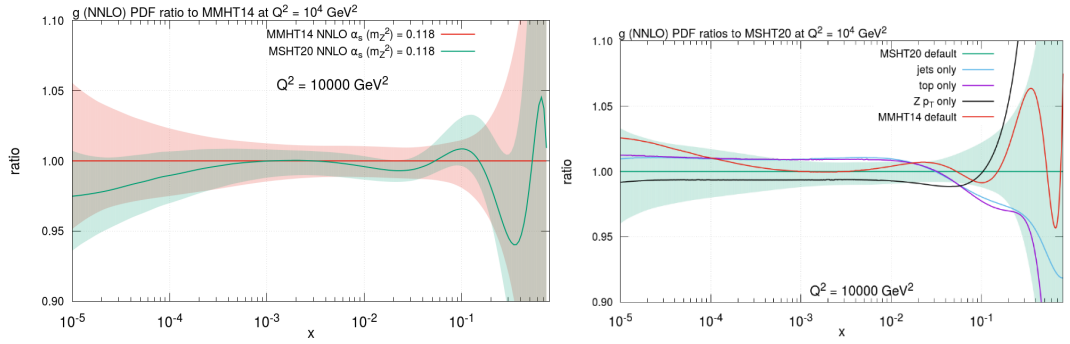

Figure 4: The MSHT20 gluon compared to MMHT14 (left); the different pulls on the MSHT20 gluon (right).

$x = 0.1$, Fig. 5 (left), due to ATLAS 7, 8 TeV data which influence PDFs similarly. There is also a significant change in the shape in valence quarks, most notably d_V, due to LHC data on W, Z and the improved parameterisation flexibility, Fig. 5 (right). The strange asymmetry is similar to MMHT14, but now is non-zero outside uncertainties. There is a change in the details of light antiquarks at high-x where constraints are weak, and a slight decrease at low x due to compensation for the increase in the strange quark. The details of the $\bar{u}, \bar{d}$ difference, shown in Fig. 6 are completely changed due to the new type of parameterisation. There is a huge increase in uncertainty at small x, and a slight tendency for negative $\bar{d} - \bar{u}$. However, a different impression is formed looking at $\bar{d}/\bar{u}$ which has small low-x uncertainty and notably the ratio $\to 1$ as $x \to 0$ to a good accuracy even without this being a constraint.

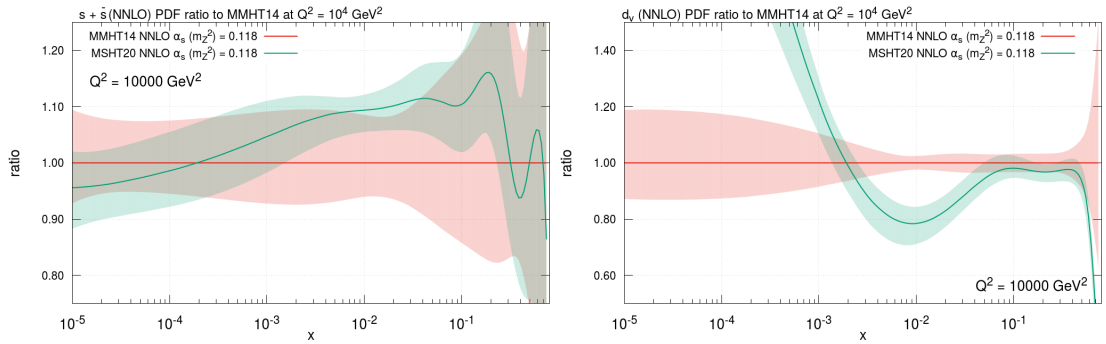

Figure 5: The MSHT20 strange quark sum (left) and down valence quark (right) compared to MMHT14.

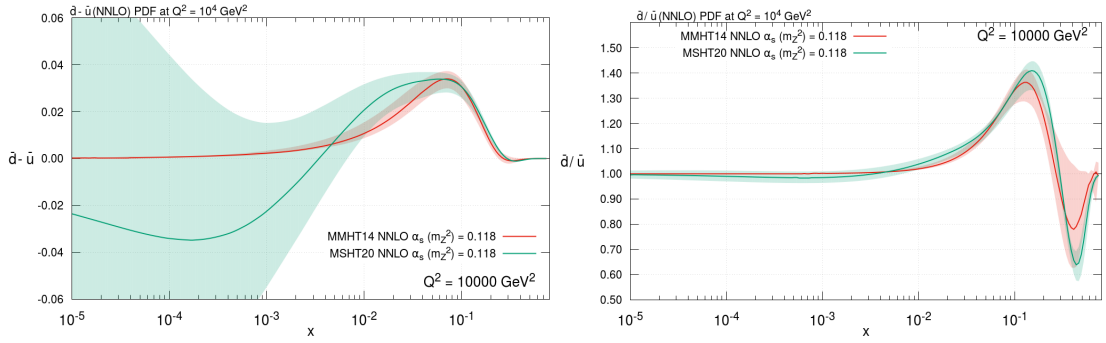

Figure 6: The MSHT20 $\bar{u}, \bar{d}$ difference compared to MMHT14.

As well as at NNLO, we also produce PDFs at NLO (and also still at LO, where the fit is very poor). We start to notice significant deterioration in fit quality for some of the precision LHC data, NNLO is now very much preferred.

The strong coupling value obtained from the analysis is $\alpha_S(M_Z^2) = 0.1174 \pm 0.0013$ [45]. There are constraints from a variety of new LHC data, but in different directions – in general jet data prefer slightly lower, while W, Z data prefer slightly higher $\alpha_S(M_Z^2)$, and no single new set constrains $\alpha_S(M_Z^2)$ more strongly than a number of older data sets. For quark masses, unlike previous results [46] which preferred lower values ($m_c^{\rm pole} \sim 1.25$ GeV), the default choice of $m_c^{\rm pole} = 1.4$ GeV is close to optimal. There is no strong pull from the default choice $m_b^{\rm pole} = 4.75$ GeV, though slightly lower values are weakly preferred [45].

5 Predictions

We show in Fig. 7 the predictions for a variety of benchmark processes. There are some changes in σ_W, σ_Z and particularly their ratio largely due to changes in strange quarks. For gluon initiated top and Higgs cross sections there is an improvement in uncertainties but the central values remain stable.

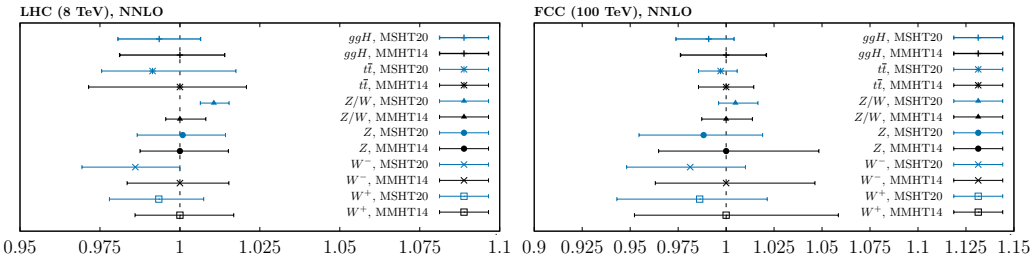

Figure 7: Predictions for benchmark processes for MMHT20 compared with those for MMHT14, for both 8 and 100 TeV colliders.

We have also produced numerous predictions for data sets not included in the fit. For example there is a good prediction for CMS 13 TeV $W+c$ data [47] which is mainly dependent on strange quarks. Single top data is not fit (since the uncertainties are much larger than PDF uncertainties), but good predictions are obtained (using [48, 49] for 13 TeV CMS data [50], as seen in Fig. 8.

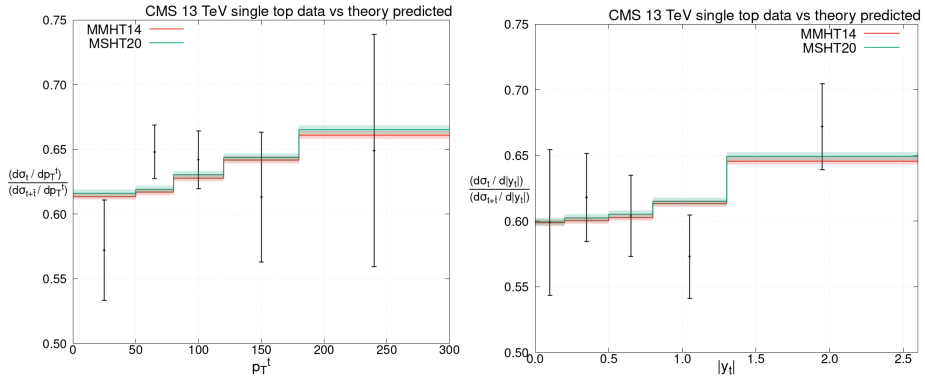

Figure 8: Predictions for single top p_T (left) and y_t (right) distributions compared to CMS data.

6 Conclusion

We have presented the MSHT20 PDF analysis. LHC data are starting to have a very significant impact on PDF extractions. Theory precision is catching up to that of data, e.g NNLO calculations for jets,differential top, $Z, W p_T$ distributions. We have also made improvements in our PDF parameterisation, which gives a better fit to data and improves some data tensions and increases some uncertainties in extreme kinematic regions. There are significant changes in the $\bar{d}, \bar{u}$ difference, in the $s + \bar{s}$ distribution and small-x $d_V(x)$ distribution for both uncertainties and central values. Generally there is stability for other PDFs, but an uncertainty reduction in PDFs/benchmark processes. Precision data and theory are causing problems in cases where correlated systematics (which increasingly dominate) are important and improved interplay between theory/experiment on these seems a priority. Additional PDFs with varying $\alpha_S(M_Z^2)$ and quark masses, have appeared, as have also the PDFs with the photon distribution [51]. Theory uncertainties on MSHT PDFs will appear, but take a little longer.

Funding information T. C. and R. S. T. thank the Science and Technology Facilities Council (STFC) for support via grant awards ST/P000274/1 and ST/T000856/1. S. B. acknowledges financial support from STFC. L. H. L. thanks STFC for support via grant award ST/L000377/1.

References

[1] S. Bailey, T. Cridge, L. A. Harland-Lang, A. D. Martin and R. S. Thorne, *Parton distributions from LHC, HERA, Tevatron and fixed target data: MSHT20 PDFs*, Eur. Phys. J. C **81**, 341 (2021), doi:10.1140/epjc/s10052-021-09057-0.

[2] R. D. Ball et al., *Parton distributions from high-precision collider data*, Eur. Phys. J. C **77**, 663 (2017), doi:10.1140/epjc/s10052-017-5199-5.

[3] T.-J. Hou et al., *New CTEQ global analysis of quantum chromodynamics with high-precision data from the LHC*, Phys. Rev. D **103**, 014013 (2021), doi:10.1103/PhysRevD.103.014013.

[4] S. Alekhin, J. Blümlein, S. Moch and R. Plačakytė, *Parton distribution functions, α_s, and heavy-quark masses for LHC Run II*, Phys. Rev. D **96**, 014011 (2017), doi:10.1103/PhysRevD.96.014011.

[5] L. A. Harland-Lang, A. D. Martin, P. Motylinski and R. S. Thorne, *Parton distributions in the LHC era: MMHT 2014 PDFs*, Eur. Phys. J. C **75**, 204 (2015), doi:10.1140/epjc/s10052-015-3397-6.

[6] R. S. Thorne and R. Roberts, *An Ordered analysis of heavy flavor production in deep inelastic scattering*, Phys. Rev. D **57**, 6871 (1998), doi:10.1103/PhysRevD.57.6871.

[7] R. S. Thorne, *Variable-flavor number scheme for next-to-next-to-leading order*, Phys. Rev. D **73**, 054019 (2006), doi:10.1103/PhysRevD.73.054019.

[8] R. S. Thorne, *Effect of changes of variable flavor number scheme on parton distribution functions and predicted cross sections*, Phys. Rev. D **86**, 074017 (2012), doi:10.1103/PhysRevD.86.074017.

[9] D. de Florian, R. Sassot, P. Zurita and M. Stratmann, *Global Analysis of Nuclear Parton Distributions*, Phys. Rev. D **85**, 074028 (2012), doi:10.1103/PhysRevD.85.074028.

[10] E. L. Berger, J. Gao, C. Sheng Li, Z. Long Liu and H. Xing Zhu, *Charm-Quark Production in Deep-Inelastic Neutrino Scattering at Next-to-Next-to-Leading Order in QCD*, Phys. Rev. Lett. **116**, 212002 (2016), doi:10.1103/PhysRevLett.116.212002.

[11] M. Goncharov et al., *Precise Measurement of Dimuon Production Cross-Sections in ν_μ Fe and $\bar{\nu}_\mu$ Fe Deep Inelastic Scattering at the Tevatron.*, Phys. Rev. D **64**, 112006 (2001), doi:10.1103/PhysRevD.64.112006.

[12] M. Aaboud et al., *Precision measurement and interpretation of inclusive W^+ , W^- and Z/γ^* production cross sections with the ATLAS detector*, Eur. Phys. J. C **77**, 367 (2017), doi:10.1140/epjc/s10052-017-4911-9.

[13] G. Aad et al., *Measurement of the cross-section and charge asymmetry of W bosons produced in proton–proton collisions at $\sqrt{s}$ =8 TeV with the ATLAS detector*, Eur. Phys. J. C **79**, 760 (2019), doi:10.1140/epjc/s10052-019-7199-0.

[14] M. Aaboud et al., *Measurement of the Drell-Yan triple-differential cross section in pp collisions at $\sqrt{s}$ = 8 TeV*, J. High Energy Phys. **12**, 059 (2017), doi:10.1007/JHEP12(2017)059.

[15] G. Aad et al., *Determination of the strange quark density of the proton from ATLAS measurements of the $W \to \ell\nu$ and $Z \to \ell\ell$ cross sections*, Phys. Rev. Lett. **109**, 012001 (2012), doi:10.1103/PhysRevLett.109.012001.

[16] J. Currie, E. W. N. Glover and J. Pires, *Next-to-Next-to Leading Order QCD Predictions for Single Jet Inclusive Production at the LHC*, Phys. Rev. Lett. **118**, 072002 (2017), doi:10.1103/PhysRevLett.118.072002.

[17] N. Kidonakis and J. F. Owens, *Effects of higher-order threshold corrections in high-E(T) jet production*, Phys. Rev. D **63**, 054019 (2001), doi:10.1103/PhysRevD.63.054019.

[18] S. Chatrchyan et al., *Measurement of Associated W + Charm Production in pp Collisions at $\sqrt{s} = 7$ TeV*, J. High Energy Phys. **02**, 013 (2014), doi:10.1007/JHEP02(2014)013.

[19] A. D. Martin, A. Mathijssen, W. Stirling, R. S. Thorne, B. Watt and G. Watt, *Extended Parameterisations for MSTW PDFs and their effect on Lepton Charge Asymmetry from W Decays*, Eur. Phys. J. C **73**, 2318 (2013), doi:10.1140/epjc/s10052-013-2318-9.

[20] H. Abramowicz et al., *Combination of measurements of inclusive deep inelastic $e^{\pm}p$ scattering cross sections and QCD analysis of HERA data*, Eur. Phys. J. C **75**, 580 (2015), doi:10.1140/epjc/s10052-015-3710-4.

[21] L. A. Harland-Lang, A. D. Martin, P. Motylinski and R. S. Thorne, *The impact of the final HERA combined data on PDFs obtained from a global fit*, Eur. Phys. J. C **76**, 186 (2016), doi:10.1140/epjc/s10052-016-4020-1.

[22] H. Abramowicz et al., *Combination and QCD analysis of charm and beauty production cross-section measurements in deep inelastic ep scattering at HERA*, Eur. Phys. J. C **78**, 473 (2018), doi:10.1140/epjc/s10052-018-5848-3.

[23] V. M. Abazov et al., *Measurement of the electron charge asymmetry in $p\bar{p} \to W + X \to e\nu + X$ decays in $p\bar{p}$ collisions at $\sqrt{s} = 1.96$ TeV*, Phys. Rev. D **91**, 032007 (2015), doi:10.1103/PhysRevD.91.032007, [Erratum: Phys. Rev. D **91**, 079901 (2015)].

[24] V. M. Abazov et al., *Measurement of the W Boson Production Charge Asymmetry in $p\bar{p} \to W + X \to e\nu + X$ Events at $\sqrt{s} = 1.96$ TeV*, Phys. Rev. Lett. **112**, 151803 (2014), doi:10.1103/PhysRevLett.112.151803, [Erratum: Phys. Rev. Lett. **114**, 049901 (2015)].

[25] T. A. Aaltonen et al., *Combination of Measurements of the Top-Quark Pair Production Cross Section from the Tevatron Collider*, Phys. Rev. D **89**, 072001 (2014), doi:10.1103/PhysRevD.89.072001.

[26] S. Chatrchyan et al., *Measurement of the $t\bar{t}$ production cross section in the dilepton channel in pp collisions at $\sqrt{s} = 8$ TeV*, J. High Energy Phys. **02**, 024 (2014), doi:10.1007/JHEP02(2014)024, [Erratum: J. High Energy Phys. **02**, 102 (2014)].

[27] R. Aaij et al., *Measurement of the forward Z boson production cross-section in pp collisions at $\sqrt{s} = 7$ TeV*, J. High Energy Phys. **08**, 039 (2015), doi:10.1007/JHEP08(2015)039.

[28] R. Aaij et al., *Measurement of forward W and Z boson production in pp collisions at $\sqrt{s} = 8$ TeV*, J. High Energy Phys. **01**, 155 (2016), doi:10.1007/JHEP01(2016)155.

[29] R. Aaij et al., *Measurement of forward $\mathrm{Z} \to \mathrm{e}^+\mathrm{e}^-$ production at $\sqrt{s} = 8$ TeV*, J. High Energy Phys. **05**, 109 (2015), doi:10.1007/JHEP05(2015)109.

[30] V. Khachatryan et al., *Measurement of the differential cross section and charge asymmetry for inclusive $\mathrm{pp} \to \mathrm{W}^{\pm} + X$ production at $\sqrt{s} = 8$ TeV*, Eur. Phys. J. C **76**, 469 (2016), doi:10.1140/epjc/s10052-016-4293-4.

[31] G. Aad et al., *Measurement of the inclusive jet cross-section in proton-proton collisions at $\sqrt{s} = 7$ TeV using 4.5 fb^{-1} of data with the ATLAS detector*, J. High Energy Phys. **02**, 153 (2015), doi:10.1007/JHEP02(2015)153, [Erratum: J. High Energy Phys. **09**, 141 (2015)].

[32] S. Chatrchyan et al., *Measurement of the Ratio of Inclusive Jet Cross Sections using the Anti-k_T Algorithm with Radius Parameters R=0.5 and 0.7 in pp Collisions at $\sqrt{s} = 7$ TeV*, Phys. Rev. D **90**, 072006 (2014), doi:10.1103/PhysRevD.90.072006.

[33] G. Aad et al., *Measurement of the transverse momentum and ϕ^*_η distributions of Drell–Yan lepton pairs in proton–proton collisions at $\sqrt{s} = 8$ TeV with the ATLAS detector*, Eur. Phys. J. C **76**, 291 (2016), doi:10.1140/epjc/s10052-016-4070-4.

[34] V. Khachatryan et al., *Measurement and QCD analysis of double-differential inclusive jet cross sections in pp collisions at $\sqrt{s} = 8$ TeV and cross section ratios to 2.76 and 7 TeV*, J. High Energy Phys. **03**, 156 (2017), doi:10.1007/JHEP03(2017)156.

[35] G. Aad et al., *Measurements of top-quark pair differential cross-sections in the lepton+jets channel in pp collisions at $\sqrt{s} = 8$ TeV using the ATLAS detector*, Eur. Phys. J. C **76**, 538 (2016), doi:10.1140/epjc/s10052-016-4366-4.

[36] M. Aaboud et al., *Measurement of top quark pair differential cross-sections in the dilepton channel in pp collisions at $\sqrt{s} = 7$ and 8 TeV with ATLAS*, Phys. Rev. D **94**, 092003 (2016), doi:10.1103/PhysRevD.94.092003.

[37] G. Aad et al., *Measurement of the double-differential high-mass Drell-Yan cross section in pp collisions at $\sqrt{s} = 8$ TeV with the ATLAS detector*, J. High Energy Phys. **08**, 009 (2016), doi:10.1007/JHEP08(2016)009.

[38] M. Aaboud et al., *Measurement of differential cross sections and W^+/W^- cross-section ratios for W boson production in association with jets at $\sqrt{s} = 8$ TeV with the ATLAS detector*, J. High Energy Phys. **05**, 077 (2018), doi:10.1007/JHEP05(2018)077.

[39] A. M. Sirunyan et al., *Measurement of double-differential cross sections for top quark pair production in pp collisions at $\sqrt{s} = 8$ TeV and impact on parton distribution functions*, Eur. Phys. J. C **77**, 459 (2017), doi:10.1140/epjc/s10052-017-4984-5.

[40] V. Khachatryan et al., *Measurement of the inclusive jet cross section in pp collisions at $\sqrt{s} = 2.76$ TeV*, Eur. Phys. J. C **76**, 265 (2016), doi:10.1140/epjc/s10052-016-4083-z.

[41] V. Khachatryan et al., *Measurement of the differential cross section for top quark pair production in pp collisions at $\sqrt{s} = 8$ TeV*, Eur. Phys. J. C **75**, 542 (2015), doi:10.1140/epjc/s10052-015-3709-x.

[42] L. A. Harland-Lang, A. D. Martin and R. S. Thorne, *The Impact of LHC Jet Data on the MMHT PDF Fit at NNLO*, Eur. Phys. J. C **78**, 248 (2018), doi:10.1140/epjc/s10052-018-5710-7.

[43] S. Bailey and L. A. Harland-Lang, *Differential top quark pair production at the LHC: Challenges for PDF fits*, Eur. Phys. J. C **80**, 60 (2020), doi:10.1140/epjc/s10052-020-7633-3.

[44] M. Aaboud et al., *Measurement of the inclusive jet cross-sections in proton-proton collisions at $\sqrt{s} = 8$ TeV with the ATLAS detector*, J. High Energy Phys. **09**, 020 (2017), doi:10.1007/JHEP09(2017)020.

[45] T. Cridge, L. A. Harland-Lang, A. D. Martin and R. S. Thorne, *An investigation of the α_S and heavy quark mass dependence in the MSHT20 global PDF analysis*, Eur. Phys. J. C **81**, 744 (2021), doi:10.1140/epjc/s10052-021-09533-7.

[46] L. A. Harland-Lang, A. D. Martin, P. Motylinski and R. S. Thorne, *Charm and beauty quark masses in the MMHT2014 global PDF analysis*, Eur. Phys. J. C **76**, 10 (2016), doi:10.1140/epjc/s10052-015-3843-5.

[47] A. M. Sirunyan et al., *Measurement of associated production of a W boson and a charm quark in proton-proton collisions at $\sqrt{s} = 13$ TeV*, Eur. Phys. J. C **79**, 269 (2019), doi:10.1140/epjc/s10052-019-6752-1.

[48] E. L. Berger, J. Gao, C.-P. Yuan and H. Xing Zhu, *NNLO QCD corrections tot-channel single top quark production and decay*, Phys. Rev. D **94**, 071501 (2016), doi:10.1103/PhysRevD.94.071501.

[49] E. L. Berger, J. Gao and H. X. Zhu, *Differential Distributions for t-channel Single Top-Quark Production and Decay at Next-to-Next-to-Leading Order in QCD*, J. High Energy Phys. **11**, 158 (2017), doi:10.1007/JHEP11(2017)158.

[50] A. M. Sirunyan et al., *Measurement of differential cross sections and charge ratios for t-channel single top quark production in proton–proton collisions at* $\sqrt{s} = 13\,TeV$, Eur. Phys. J. C **80**, 370 (2020), doi:10.1140/epjc/s10052-020-7858-1.

[51] T. Cridge, L. A. Harland-Lang, A. D. Martin and R. S. Thorne, *QED parton distribution functions in the MSHT20 fit*, Eur. Phys. J. C **82**, 90 (2022), doi:10.1140/epjc/s10052-022-10028-2.